Annals of Biomedical Engineering, Vol. 28, pp. 160–167, 2000
Printed in the USA. All rights reserved.

0090-6964/2000/28(2)/160/8/$15.00
Copyright © 2000 Biomedical Engineering Society

Experimental Evaluation of a Model for Oxygen Exchange in a Pulsating Intravascular Artificial Lung

WILLIAM J. FEDERSPIEL,[1,2,3] TODD J. HEWITT,[2] and BRACK G. HATTLER[1]

[1]McGowan Center for Artificial Organ Development, Department of Surgery, [2]Department of Bioengineering, and [3]the Department of Chemical Engineering, University of Pittsburgh, Pittsburgh, PA

(Received 3 March 1999; accepted 10 November 1999)

Abstract—Intravascular oxygenation and carbon dioxide removal remains a potentially attractive means for respiratory support in patients with acute or chronic respiratory failure. Our group has been developing an intravascular hollow fiber artificial lung that uses a pulsating balloon located within the fiber bundle to augment gas transfer. We previously reported on a simple compartmental model for simulating O_2 exchange in pulsating intravascular artificial lungs. In this study we evaluate the O_2 exchange model with gas exchange and PO_2 measurements performed on an idealized intravascular artificial lung (IIVAL) tested in a water perfusion loop. The IIVAL has well-defined bundle geometry and can be operated in balloon pulsation mode, or a steady perfusion mode for determining the mass transfer correlation required by the model. The O_2 exchange rates and compartmental O_2 tensions measured with balloon pulsation in the IIVAL are within 10% of model predictions for flow and pulsation conditions relevant to intravascular oxygenation. The experiments confirmed that a significant buildup of PO_2 occurs within the fiber bundle, which reduces the O_2 exchange rate. The agreement between experiments and predictions suggests that the model captures the cardinal processes dictating gas transfer in pulsating intravascular artificial lungs. © *2000 Biomedical Engineering Society.*
[S0090-6964(00)00402-1]

Keywords—Respiratory support, Artificial lung, Intravenous oxygenation, Hollow fibers, Gas transfer, Gas exchange, IMO.

INTRODUCTION

Intravenous artificial lungs or oxygenators may provide an effective means of supplementing respiratory support in patients with acute respiratory failure.[3,7,9,12] The concept involves placing a bundle of hollow fiber membranes within the vena cava by insertion through the femoral vein in the leg.[9] The fiber bundle is manifolded to gas supply and removal lines leading outside the body, which create a sweep flow of pure O_2 through the fibers. Thus the fiber membranes supply O_2 and remove CO_2 before blood flows to the natural lungs, which then transfer whatever additional O_2 and CO_2 they can. Our group has been actively developing an intravenous lung assist device that uses a pulsating balloon centrally located within the fiber bundle to enhance gas transfer.[2–5] The fiber bundle, made by wrapping hollow fiber fabric around the inflated balloon,[4] is intentionally smaller than vessel lumen size and allows a shunt flow of blood past the device. Enhanced gas transfer occurs as the central balloon rhythmically inflates and deflates to draw blood from the shunt flow across the fiber membranes in a cross flow (i.e., perpendicular to fiber axes), achieving greater relative velocities past the fibers than would exist without balloon pulsation. Effective use of the pulsating balloon results in transfer levels at or above our target of 50% of basal metabolic requirements[3] and nearly twice that of the clinically tested IVOX intravascular oxygenator.[1,9]

We previously developed a mathematical model for oxygen exchange in a pulsating intravascular lung as a tool for understanding the mechanisms by which balloon pulsation enhances gas exchange in our pulsating artificial lung and to help guide development efforts towards a maximally effective device.[6] The model built on and extended other transport models for artificial lungs developed by Niranjan *et al.*,[10] Makarewicz and Mockros,[8] Vaslef *et al.*,[13,14] and Nodelman *et al.*[11] These previous models provide a useful perspective on gas exchange in static artificial lungs, but none were directly applicable to a balloon-pulsating intravascular lung. Our model adopted a simple lumped compartment perspective, with gas exchange at the fibers dictated by a mass transfer correlation. Dynamic simulations based on the model helped elucidate the interplay between geometric design parameters of the bundle and the balloon, balloon pulsation dynamics, shunt flow past the oxygenator, and device O_2 gas transfer. The O_2 transfer rates predicted by the model, using an average of the cross-flow mass transfer correlations found in the literature, were reasonably consistent with O_2 transfer rates exhibited by recent prototypes.[6] Nevertheless, the available literature corre-

Address correspondence to William J. Federspiel, Room 428, Biotechnology Center, 300 Technology Dr., University of Pittsburgh, Pittsburgh, PA 15219. Electronic mail: federspielwj@msx.upmc.edu

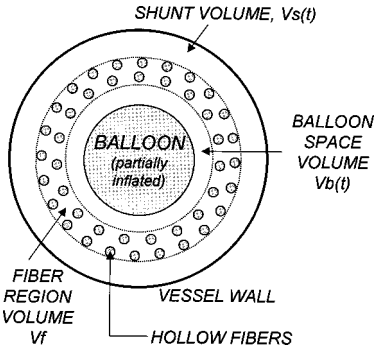

FIGURE 1. Cross-sectional view of compartments in the oxygen exchange model.

lations for mass transfer in cross flow vary, and the agreement between model predictions and prototype exchange performance may have been fortuitous based on the use of an average mass transfer correlation. Furthermore, not all important aspects of the model were tested by the comparisons to existing prototype data.

In this study we further evaluate our model of O_2 exchange in a pulsating intravascular artificial lung by water perfusion experiments on an idealized intravascular artificial lung (IIVAL), which has a well-defined fiber bundle geometry, the parameters of which are key inputs to the exchange model. Using the IIVAL we could directly measure the steady flow mass transfer correlation for the fiber bundle, then perform dynamic experiments with the pulsating balloon and compare measured gas transfer rates with those predicted using the model with this mass transfer correlation. One of the more interesting phenomena predicted by the model, and which we wanted to confirm by experiments with the IIVAL, is that a buildup in PO_2 within the fiber bundle occurs, which reduces the exchange rate of the pulsating intravascular lung. The significance of our results goes beyond its immediate application to the intravascular lung, and may find application in the development of other next generation intracorporeal and extracorporeal artificial lungs (i.e., devices not yet in clinical use), where active mechanical means like our balloon are exploited for improving gas exchange performance.

MATHEMATICAL MODEL

The oxygen exchange model for the pulsating intravascular lung is described fully in Hewitt *et al.*[6] and is only briefly described here for completeness. The model views the pulsating intravascular oxygenator as three interacting and well-mixed lumped compartments, as illustrated in the cross-sectional view in Fig. 1. The shunt (*s*) volume represents the annular volume of fluid between the fiber bundle and the vessel wall, through which flow past the fiber bundle occurs in the absence of balloon pulsation (i.e., a shunt flow). Its volume, $Vs(t)$, varies with time to accommodate the displaced fluid with each balloon inflation. The fiber (*f*) region volume is the time-invariant annular volume, V_f, between the inflated balloon and the shunt compartment, and contains the hollow fiber membranes at a given packing density. The balloon inflates and deflates within the balloon space (*b*) volume. Its time-varying volume, $V_b(t)$, maximally fills with fluid when the balloon deflates, and empties when the balloon inflates.

The pulsation of the balloon filling and emptying within the balloon space volume drives a time dependent convective flow, $Q_b(t)$, between compartments, which is the sole means by which these compartments communicate. Venous flow is delivered to the shunt compartment at a longitudinal steady flow rate of Q_L and at a venous level of inlet P_{O_2} (P_{in}). The balloon driven convective flow during deflation draws some of the shunt fluid into the fiber and balloon space regions, where its P_{O_2} increases due to gas exchange with the fibers. The instantaneous rate of O_2 exchange in the fiber region is given by

$$\dot{V}O_2(t) = K(t)A[\overline{P_g} - P_f(t)],$$

where K is a mass transfer coefficient, A is the fiber membrane surface area, $\overline{P_g}$ is the average O_2 partial pressure in the gas flowing through the fiber membranes, and P_f is the O_2 tension of the fluid within the fiber compartment. Inflation of the pulsating balloon sends fluid back into the shunt volume where it mixes with the existing shunt fluid, arriving and leaving the shunt compartment at the longitudinal flowrate Q_L. The unsteady mass balances describing the time varying O_2 tensions in each compartment (P_s, P_f, and P_b) form a system of first order differential equations, whose solution predicts the dynamics of O_2 tension and overall O_2 exchange during balloon pulsation.

The mass transfer coefficient, *K*, depends on the instantaneous flowrate through the fiber bundle, $Q_b(t)$, the fiber bundle geometry, and O_2 solubility and diffusivity parameters. In our previous application of the model, *K* was specified using a dimensionless Sherwood number correlation averaged from those available in the literature for cross flow through fiber beds.[6] In this study, we more directly test the model by determining a mass transfer correlation for the annular fiber bundle of an idealized intravascular artificial lung (IIVAL), then compare model predictions with measurements of gas exchange with dynamic balloon pulsation. The relevant apparatus and methods are described below.

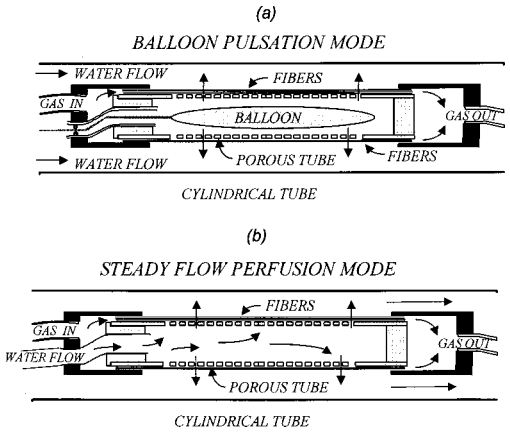

FIGURE 2. The idealized intravascular artificial lung (IIVAL): (a) Pulsating balloon used in the central porous tube; (b) steady flow perfusion mode without the pulsating balloon.

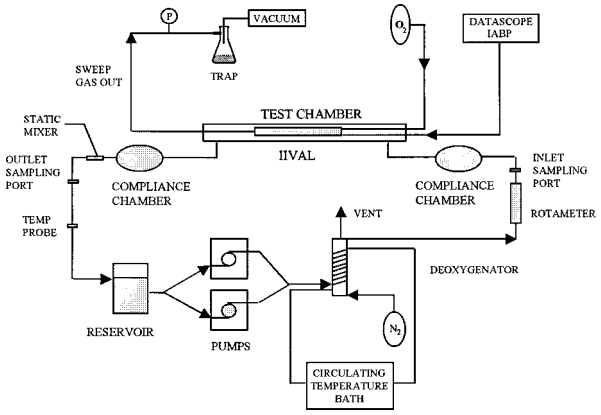

FIGURE 3. Gas exchange characterization circuit used for steady flow and dynamic testing of the IIVAL.

EXPERIMENTAL APPARATUS AND METHODS

The apparatus specifically developed to test the O_2 exchange model was an idealized intravascular artificial lung (IIVAL), as shown schematically in Fig. 2(a). The IIVAL consisted of an annular fiber bundle with well defined inner and outer diameters (1.50 and 3.15 cm, respectively) and length (25 cm), constructed by wrapping a hollow fiber fabric (Celgard×30–240 array at 35 fibers/in. Charlotte, NC) around a thin-walled central porous tube, with the hollow fiber axes parallel to the porous tube axis. A polyurethane balloon (40 m*l* volume capacity) from an intra-aortic balloon catheter (Datascope, Fairfield, NJ) was placed within the central porous tube and connected to a Datascope 90 intra-aortic balloon pump console, which pulsated the balloon with helium at rates varying up to 180 beats/min, but not with full inflation/deflation above 120 bpm (see Results and Discussion). The ends of the annular fiber bundle were epoxied into mating annular endcaps using a process that ensured the fiber lumens remained patent. One endcap was connected to an O_2 source (gas in), while the opposite endcap was connected to a vacuum source (gas out) used to drive the flow of 100% O_2 sweep gas through the fibers at slightly subatmospheric pressure. The annular fiber bundle and endcap assembly was mounted in the center of a larger 3.8 cm ID plexiglass cylindrical tube, which served as the model vessel for the IIVAL.

The complete IIVAL test chamber (fiber unit and tube) was connected through inlet and outlet flow ports at each end to a gas exchange characterization circuit (Fig. 3). The circuit consisted of a reservoir and dual centrifugal pump system that perfused distilled water at controllable steady flowrates (representing the longitudinal flowrate Q_L in the model) through the IIVAL test chamber. Compliance chambers were included immediately upstream and downstream of the IIVAL test chamber to reduce the pressure load on the pulsating balloon within the IIVAL. The compliance bags essentially accommodate the volume changes associated with the time varying shunt compartment, which in the model consists of the fixed volume between the fiber bundle and vessel wall and the volume of water displaced by the balloon. Relative to this time-varying shunt volume the longitudinal flowrate, Q_L, is a constant, consistent with the model formulation. An integral heat exchanger maintained water temperature in the circuit at 37 °C and a deoxygenator module (standard clinical blood oxygenator using N_2 sweep gas) just upstream of the test chamber was used to set the PO_2 of the inlet stream to 40 mm Hg. Fluid samples were taken immediately before and after the test chamber and analyzed using a Radiometer ABL 330 blood gas analyzer for determination of PO_2. The steady state O_2 exchange rate, $\dot{V}O_2$, was computed using

$$\dot{V}O_2 = \alpha_w Q_L (P_w^{\text{out}} - P_w^{\text{in}}),$$

where α_w is the O_2 solubility in water ($\alpha_w = 3.16 \times 10^{-4}$ ml O_2/cm^3/cm Hg), Q_L is the steady flowrate (longitudinal flowrate) through the test section, and P_w is the PO_2 in the water measured at the outlet or inlet of the test section, as noted.

The IIVAL was designed to also operate in a steady flow perfusion mode for determination of a mass transfer correlation for the fiber bundle, as required for the model. In the steady flow perfusion mode, the balloon within the IIVAL was removed and the inlet stream to the test chamber diverted directly into the central porous tube within the fiber bundle [Fig. 2(b)]. The fluid then flowed radially outward through the fiber bundle and into the plexiglass cylindrical tube surrounding the IIVAL, prior to leaving the test chamber. At flowrates varying from 1 to 6 L/min, the O_2 exchange rate was computed and the mass transfer coefficient determined using

$$K = \frac{\dot{V}O_2}{A\Delta P_{lm}}$$

where A is the fiber membrane surface area, ΔP_{lm} is the log mean O_2 partial pressure difference between the gas flowing through the fibers, and the water flowing through the fiber bundle. The log mean partial pressure difference accounts for the exponential approach of gas and water phase PO_2 as fluid flows from inside to outside the fiber bundle, and is given by

$$\Delta P_{lm} = \frac{(\overline{P}_g - P_w^{in}) - (\overline{P}_g - P_w^{out})}{\ln^{\overline{P}_g - P_w^{in}}/_{\overline{P}_g - P_w^{out}}},$$

where $\overline{P}_g$ is the average O_2 partial pressure within the fibers, computed as the average of total gas pressure measured at the inlet and outlet endcaps (i.e., the sweep gas is negligibly diluted during fiber transit). In our application the log mean PO_2 difference was always close to the direct difference, $\overline{P}_g - \overline{P}_w$, where $\overline{P}_w$ is the average of P_w^{in} and P_w^{out}.

The mass transfer coefficient was cast into a dimensionless Sherwood number correlation, $Sh = aRe^bSc^{1/3}$, required for the model simulations. The Sherwood number was defined by $Sh = Kd_f/\alpha_w D_w$, where d_f is the fiber diameter, and D_w is the diffusion coefficient of O_2 in water ($D_w = 2.8\times10^{-5}$ cm^2/s). The Reynolds number was computed as $Re = Vd_f/\nu$, where V is the mean interstitial flow velocity and ν is the kinematic viscosity of water (7.0×10^{-3} cm^2/s). The interstitial velocity V depends on the outward radial flowrate, Q_r, through the fiber bundle and the average cross-sectional area through which the fluid flows. For a fiber bundle with inner diameter, d_i, outer diameter, d_o, length, L, and porosity (void volume to total volume), ϵ, we computed the mean interstitial velocity using $V = Q_r/(\pi/2)(d_i + d_o)L\epsilon$. The radial flowrate through the bundle was varied between 1 and 6 L/min, and the computed Sherwood numbers were fit to the dimensionless correlation to yield the a and b correlation parameters. Since only one fluid was used, the Schmidt number ($Sc = \nu/D_w$) was a constant.

Table 1 summarizes the pertinent geometrical parameters of the IIVAL and functional parameters associated with its testing. The parameters that are direct input to the simulation model of O_2 exchange are noted.[6]

TABLE 1. Geometric and functional parameters of the IIVAL.

Description	Symbol	Value
Outer diameter of hollow fiber[a]	d_f	300 μm
Inner diameter of fiber bundle (inflated balloon diameter)[a]	d_i	1.5 cm
Outer diameter of fiber bundle[a]	d_o	3.15 cm
Diameter of vessel[a]	d_v	3.80 cm
Length of fiber bundle[a]	L	25 cm
Porosity of fiber bundle[a]	ϵ	0.68
Membrane surface area	A	0.54 m^2
Number of fibers		~2300
Average gas side pressure[a]	$\overline{P}_g$	750 mm Hg
Inlet water O_2 partial pressure[a]	P_w^{in}	40 mm Hg
Longitudinal flowrate[a]	Q_L	varied
Balloon pulsation frequency[a]	F	varied

[a]Denotes parameters which are direct input to the O_2 exchange simulation model.

RESULTS AND DISCUSSION

Steady flow radial perfusion through the fiber bundle of the idealized intravascular artificial lung (IIVAL) produced larger Sherwood numbers than the average literature correlation for mass transfer in cross flow to fiber beds (Fig. 4). A nonlinear regression of the Sherwood number data indicated a specific correlation given by $Sh = 0.71Re^{0.51}Sc^{1/3}$, compared to the average of the literature correlations given by $Sh = 0.52Re^{0.52}Sc^{1/3}$.[6] The Reynolds number dependence of the two correlations is comparable, which, as would be expected, suggests comparable mechanisms of convection and diffusion associated with transfer from the fibers. Nevertheless, the Sherwood number for the IIVAL bundle is nearly 50% larger than the average cross-flow correlation (a proportionality constant of 0.71 vs 0.52). The IIVAL bundle is fabricated using a fiber fabric that has a highly uniform fiber spacing (at 35 fibers/in.). The larger Sherwood number may reflect a preferable fiber distribution in the IIVAL bundle associated with use of the fiber fabric. This appears consistent with findings of Wickramasinghe *et al.*,[15] who reported that the Sherwood number for fiber beds made from fiber fabric approached that of meticulously handmade uniform fiber banks.

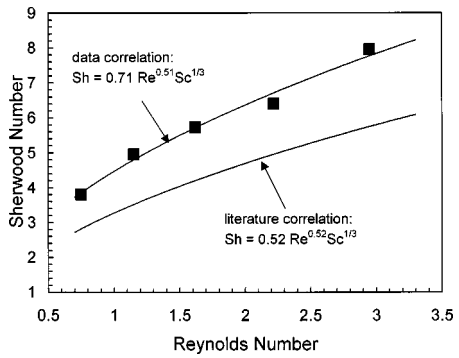

FIGURE 4. Dimensionless mass transfer correlation for steady radial flow through fiber bundle of the IIVAL. Flowrate varied from 1 to 6 L/min; values for other parameters in Table 1.

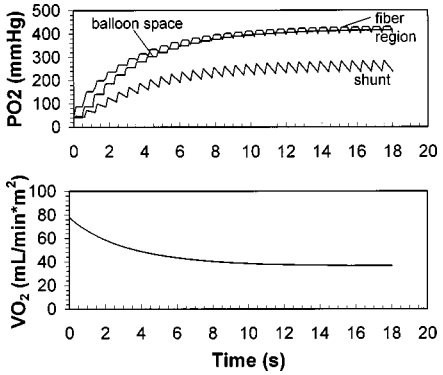

FIGURE 5. Simulations of compartmental PO_2 (upper panel) and cycle-averaged $\dot{V}O_2$ (lower panel) in water for the idealized intravascular artificial lung. Longitudinal flowrate: $Q_L = 3.1$ L/min; pulsation frequency: $F = 100$ bpm; values for other parameters in Table 1.

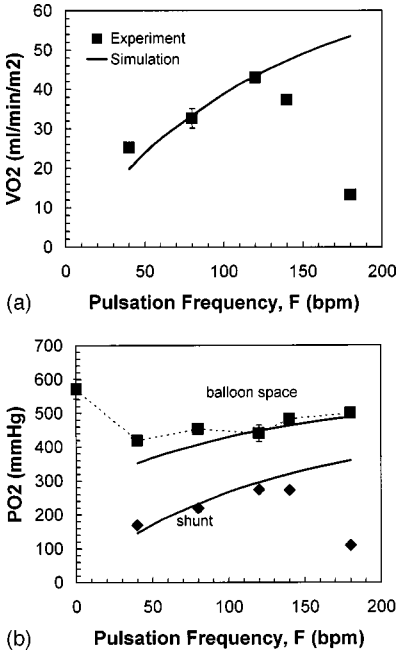

FIGURE 6. Comparison of measured (symbols) and predicted (line) O_2 exchange performance in water for the IIVAL over a relevant range of balloon pulsation, for fixed longitudinal flowrate ($Q_L = 3$ L/min): (a) O_2 exchange rate normalized to fiber surface area; (b) PO_2 values in the balloon space and shunt volume regions. Symbols represent means ±S.D. of 2–3 measurements, but only S.D. bars greater than symbol size are seen.

The Sherwood number correlation determined above becomes input to the O_2 exchange model. Dynamic simulations of the compartmental PO_2 values (upper panel) and the cycle-average $\dot{V}O_2$ (lower panel) for the IIVAL during water perfusion are shown in Fig. 5. The balloon pulsates in an impulse mode to simulate the motion imparted by the Datascope console,[6] and the functional dependencies for $Q_b(t)$, $Vb(t)$, and $Vs(t)$ in this mode are given in Hewitt *et al.* All compartments start with an initial O_2 tension of 40 mm Hg, which is also the O_2 tension in the inlet flow. The steady longitudinal flowrate is $Q_L = 3.1$ L/min and the balloon pulsation frequency is $F = 100$ bpm; all other input simulation parameters are listed in Table 1. The compartments reach an oscillatory steady state within a few seconds, when the cycle-average exchange rate becomes constant and PO_2 values fluctuate about a constant mean. The simulations here exhibit the same qualitative behavior as those reported in the original application of the O_2 exchange model.[6] Most notably, the dynamics of exchange and mixing between the longitudinal shunt flow and the balloon-generated flow lead to a build up of PO_2 within the fiber region and the balloon space region. The PO_2 buildup reduces the O_2 exchange rate by virtue of a diminished PO_2 drop between the fibers and the surrounding fluid. The model assumes that fluid leaving the fiber region during balloon inflation mixes perfectly with the fluid in the shunt volume. Thus, fluid drawn back into the fiber bundle during balloon deflation will have fluid elements that have already been within the fiber bundle, and the fraction of such elements can be significant when the balloon generated flowrate is comparable to or exceeds the longitudinal flowrate. For perfect mixing compartments as assumed in our model, the fraction of fluid elements returning to the fiber bundle is approximately given by the ratio of the average balloon generated flowrate during inflation to the sum of longitudinal flowrate plus balloon generated flowrate. Assuming a 40 ml balloon at 120 bpm, and a Q_L of 3 L/min, the ratio of returning fluid elements is approximately 76%. Physically these returning fluid elements contribute to a greater PO_2 buildup than would otherwise exist within the fiber bundle and to a reduction in the O_2 exchange rate. The prediction and magnitude of the PO_2 buildup directly rests on the interaction between compartments prescribed by the model, and hence was one of the principal features we wanted to explore with the experiments on the IIVAL.

The measured and predicted O_2 exchange rates in water for the idealized intravascular artificial lung are compared in Fig. 6(a) over a relevant range of balloon pulsation frequencies, for a fixed longitudinal flowrate of $Q_L = 3$ L/min. The model accounts only for gas exchange engendered by balloon pulsation. Accordingly, the experimental exchange rates seen in Fig. 6(a) are corrected to approximate balloon engendered exchange only, by subtracting out the IIVAL O_2 exchange rate with no balloon pulsation. The exchange rate of the IIVAL with no pulsation at this flowrate is less than 5 ml/min/m^2, and hence the correction only represents an 11% adjustment to the maximum $\dot{V}O_2$ values. The measured and predicted $\dot{V}O_2$ increase with balloon pulsation rate and

are in good agreement up to about 120 bpm. Beyond 120 bpm the measured and predicted exchange deviate significantly. For the IIVAL (as for any real pulsating device) a ''critical frequency'' exists above which the balloon no longer completely fills and empties due to the pneumatic resistance of the helium gas pathway used to fill the balloon combined with the pressure load on the balloon. We performed a separate test of balloon filling and emptying in the IIVAL using a plethysmographic chamber designed to determine this critical frequency. These tests verified that the IIVAL has a critical frequency of 120 bpm with the balloon drive system used in these experiments. Accordingly, the measured O_2 exchange rate drops sharply beyond 120 bpm because convective flow generated by the balloon diminishes as the balloon no longer completely fills and empties. The predicted O_2 exchange rate continues to increase beyond 120 bpm because the model assumes complete balloon filling and emptying at all pulsation rates. Clearly, the actual reduced amplitude of balloon pulsation beyond the critical frequency could be measured with plethysmography and incorporated in the model simulations. Doing so would improve the agreement between experiment and simulations but would not make the model more useful for our purposes. The model exists principally to explore how gas transfer varies with changes in geometric design variables of the fiber bundle and the balloon. The critical frequency is set by the pneumatic circuit supplying helium to the balloon and by the balloon drive console. In ultimate application of a pulsating intravascular lung these features would be optimized or chosen to allow full balloon pulsations at the desired frequency.

The simulations indicate that the O_2 exchange rate in steady state is reduced by a significant buildup of PO_2 in the fiber and balloon space compartments (Fig. 5). Accordingly, an important test of the model would be to directly compare predicted PO_2 values in the fiber and balloon space compartment with experimental measurements. The degree to which the predicted O_2 exchange rate agreed with experiments [Fig. 6(a)] would suggest that these elevated PO_2 values should be seen if the model reasonably reflects the dynamic processes occurring. Fluid samples from within the fiber volume region were not feasible, but we could guide a thin sampling catheter next to the balloon for PO_2 measurement in the balloon space volume during balloon pulsation. The PO_2 measured in the outlet sample provides the comparison with shunt volume PO_2. Figure 6(b) shows that the experimentally measured PO_2 values in the balloon space and shunt volume regions are in good agreement with their respective predicted values. Above the critical frequency of 120 bpm, the measured O_2 tension in the shunt volume drops as the balloon can no longer fully fill and empty, and balloon convective flow diminishes. The predicted shunt O_2 tension does not fall because the balloon in the model maintains increasing convective flow with increasing pulsation rate. The reduction in balloon convective flow has little effect on the measured O_2 tension in the balloon space compartment. This is so because O_2 exchange at the fibers also decreases as balloon convective flow decreases.

An appreciable deviation between theory and experiment occurs for the balloon space O_2 tension in the limit of zero balloon pulsation rates. In this limit the model has no communication between the balloon space and shunt regions and no O_2 exchange at the fibers. Thus the balloon space region in the model remains at the venous value of O_2 tension presumed for the initial condition. In contrast the IIVAL exhibits a small O_2 exchange rate with no balloon pulsation, which is about an order-of-magnitude less than that with pulsation. The O_2 exchange at zero pulsation results from a combination of diffusion from the fiber bundle with some longitudinal flow penetrating the fiber bundle. The fiber region thus saturates with O_2 until its PO_2 approaches the average partial pressure of O_2 gas in the fibers. This explanation most likely accounts for the substantially elevated PO_2 seen in the balloon space region ($P_b = 580$ mm Hg) compared to predictions, whereas at higher balloon pulsation rates data and theory converge.

The measured and predicted $\dot{V}O_2$ and PO_2 values for the IIVAL are compared in Fig. 7 over a relevant range of longitudinal (shunt) water flowrates, for a fixed balloon pulsation rate of $F = 100$ bpm. Measurement and prediction show comparable trends toward greater O_2 exchange rates with increasing longitudinal flowrate [Fig. 7(a)]. Balloon convective flowrate is constant (F fixed), and so the increased O_2 exchange results from a decreased O_2 buildup within the fiber bundle, as more ''fresh'' (i.e., venous) fluid is available for mixing with the balloon generated flow. This explanation is supported by both the measured and simulated PO_2 values in the balloon space region [Fig. 7(b)], which decrease with increasing longitudinal flowrate. Figure 7(b) does indicate that the measured PO_2 in the balloon space region lies slightly above predictions, while that in the shunt volume lies below. Better agreement was seen in the earlier series of experiments in which balloon pulsation was varied at fixed longitudinal flowrate (Fig. 6). That the PO_2 in the balloon space region lies above predictions, while the shunt PO_2 lies below, may suggest some reduced level of mixing in the flow experiments compared to the pulsation experiments. Nevertheless, theory and predictions still show comparable trends and agree to within 10%.

CONCLUSIONS

Oxygen exchange in the idealized intravascular artificial lung was well predicted, to within 10%, by simula-

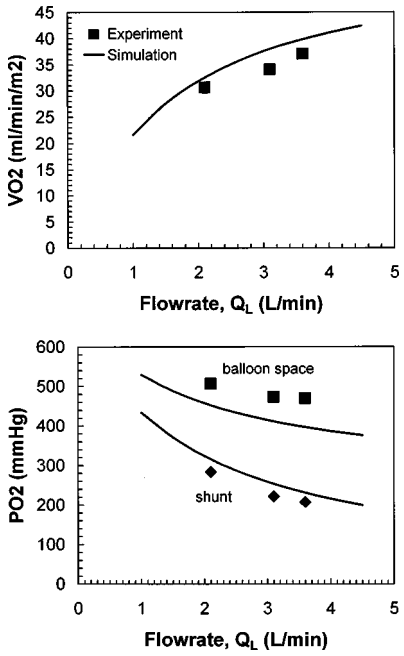

FIGURE 7. Comparison of measured (symbols) and predicted (line) O_2 exchange performance in water for the IIVAL over a relevant range of longitudinal flowrates for fixed balloon pulsation rate (F=100 bpm): (a) O_2 exchange rate normalized to fiber surface area; (b) PO_2 values in the balloon space and shunt volume regions. Symbols represent means ±S.D. of 2–3 measurements, but only S.D. bars greater than symbol size are seen.

tions based on our simple lumped compartment model. The experiments and model simulations taken together provide important insight into the mechanisms underlying gas exchange performance and the cardinal factors that dictate exchange in pulsating intravascular oxygenators. The principal role of the pulsating balloon is to take the longitudinal flow, which runs predominantly parallel to the fibers and may even largely bypass the fibers, and transform it into cross flow through the fiber bundle interstices. Our quantitative model for O_2 exchange in the pulsating intravascular lung originally arose from a desire to understand how effectively such devices exploit the efficiencies of cross flow. Our simulations, now confirmed by experiments, have identified an important feature of gas exchange in the pulsating intravascular lung. Although mass transfer occurs by cross flow to the fibers, some of the effectiveness of cross flow is lost due to a buildup of PO_2 within the fiber bundle and a diminished driving force for gas exchange. The buildup occurs in the presence of perfect mixing in each of the compartments, as assumed by the model, including perfect mixing of the fluid displaced by the inflating balloon with the shunt flow. Increasing the frequency of pulsation helps. But with a fixed longitudinal flowrate that is generally smaller than the balloon convective flowrate, a buildup of PO_2 and loss of gas exchange is inevitable.

For simplicity the experiments done here used water as the blood analog. Our original modeling studies indicated that in blood, hemoglobin does ''buffer'' the buildup of PO_2 within the fiber and balloon space regions compared to the buildup in water. For the simulation case presented in Hewitt *et al.*[6] for example, the PO_2 within the fiber bundle only reached 80–90 mm Hg for blood compared to 400–500 mm Hg in water under otherwise comparable conditions. Nevertheless, the O_2 exchange rate in blood drops about the same relative magnitude as that in water.[6] Clearly, the drop in exchange in blood is not due to a loss of driving force, but occurs because the increased saturation of hemoglobin at an O_2 tension of 80–90 mm Hg reduces the effective solubility of O_2 in blood, another key determinant of the O_2 exchange rate. Validating the exchange model in water as done here may actually be a better test of the model. It decouples the validation from any concern about how the model treats the more complicated interaction of O_2 and blood, including the PO_2 dependent, increased effective solubility of O_2 in the presence of hemoglobin. The model focuses on balloon-generated convection, transfer from the fibers, and the mixing within compartments. Had the experiments not shown a comparable buildup of PO_2 in water, serious concerns would arise about the mixing assumptions and the compartmental interaction prescribed in the model. Indeed these are principal features that dictate the physics of convection and exchange in the model. Accordingly, the relatively good agreement between experiments and simulations indicates that the model reasonably reflects the gas exchange processes underlying pulsating intravascular artificial lungs.

Our studies may find application in other areas of artificial lung development, and possibly other areas involving membrane modules. A current trend exists in artificial lungs towards respiratory support devices that can be made smaller and more efficient for extracorporeal, paracorporeal, or intracorporeal application.[3] The active mixing and enhanced gas transfer associated with pulsating balloons within a fiber bundle make these designs potentially attractive candidates. Our model represents a relatively simple design tool which can help guide development of these next generation artificial lungs.

ACKNOWLEDGMENTS

This work was supported by the U.S. Army Medical Research, Development, Acquisition, and Logistics command under prior Contract No. DAMD17-94-C-4052 and current Grant No. DAMD17-98-1-8638. The views,

opinions, and/or findings contained in this report are those of the authors and should not be construed as an official Department of the Army position, policy, or decision unless so designated by other documentation. The generous support of the McGowan Foundation is also appreciated. A Special Opportunity Award from the Whitaker Foundation provided funding for the graduate education of T. J. Hewitt. We thank Sue Wanant for her technical assistance.

REFERENCES

[1] Conrad, S. A. *et al.* Major findings from the clinical trials of the intravascular oxygenator. *Artif. Organs* 18:846–863, 1994.

[2] Federspiel, W. J., T. J. Hewitt, M. S. Hout, F. R. Walters, L. W. Lund, P. Sawzik, G. D. Reeder, H. S. Borovetz, and B. G. Hattler. Recent progress in engineering the Pittsburgh Intravenous Membrane Oxygenator. *ASAIO J.* 42:M435–M442, 1996.

[3] Federspiel, W. J., P. Sawzik, H. Borovetz, G. D. Reeder, and B. G. Hattler. Temporary support of the lungs—The artificial lung, edited by D. K. C. Cooper, L. W. Miller, G. A. Patterson. The Transplantation and Replacement of Thoracic Organs, Boston: Kluwer Academic, 1996, p. 824.

[4] Federspiel, W. J., M. S. Hout, T. J. Hewitt, L. W. Lund, S. A. Heinrich, P. Litwak, F. R. Walters, G. D. Reeder, H. S. Borovetz, and B. G. Hattler. Development of a low flow resistance intravenous oxygenator. *ASAIO J.* 43:M725–M730, 1997.

[5] Hattler, B. G., G. D. Reeder, P. J. Sawzik, L. W. Lund, F. R. Walters, A. S. Shah, J. Rawleigh, J. S. Goode, M. Klain, and H. S. Borovetz. Development of an intravenous membrane oxygenator: enhanced intravenous gas exchange through convective mixing of blood around hollow fiber membranes. *Artif. Organs* 18:806–812, 1994.

[6] Hewitt, T. J., B. G. Hattler, and W. J. Federspiel. A mathematical model of gas exchange in an intravenous membrane oxygenator. *Ann. Biomed. Eng.* 26(1):166–178, 1998.

[7] High, K. M., M. T. Snider, R. Richard, G. B. Russell, J. K. Stene, D. B. Campbell, T. X. Aufiero, and G. A. Thieme. Clinical trials of an intravenous oxygenator in patients with adult respiratory distress syndrome. *Anesthesiology* 77:856–863, 1992.

[8] Makarewicz, A. J., and L. F. Mockros. Modeling oxygen transfer to blood from crossflow membrane oxygenators. *ASME: Bioengineering Division* 29:467–468, 1995.

[9] Mortensen, J. D. Intravascular oxygenator: A new alternative method for augmenting blood gas transfer in patients with acute respiratory failure. *Artif. Organs* 16:75–82, 1992.

[10] Niranjan, S. C., J. W. Clark, K. Y. San, J. B. Zwischenberger, and A. Bidani. Analysis of factors affecting gas exchange in intravascular blood gas exchanger. *J. Appl. Physiol.* 77:1716–1730, 1994.

[11] Nodelman, V., H. Baskaran, and J. S. Ultman. Enhancement of O_2 and CO_2 transfer through microporous hollow fibers by pressure cycling. *Ann. Biomed. Eng.* 26:1044–1054, 1998.

[12] Tao, W., and J. B. Zwishenberger. Intracorporeal gas exchange: Taking further steps. *ASAIO J.* 44(3):224–226, 1998.

[13] Vaslef, S. N., L. F. Mockros, K. E. Cook, R. J. Leonard, J. C. Sung, and R. W. Anderson. Computer-assisted design of an implantable, intrathoracic artificial lung. *Artif. Organs* 18(11):813–817, 1994.

[14] Vaslef, S. N., L. F. Mockros, R. W. Anderson, and R. J. Leonard. Use of a mathematical model to predict oxygen transfer rates in hollow fiber membrane oxygenators. *ASAIO J.* 40:990–996, 1994.

[15] Wickramasinghe, S. R., M. J. Semmens, and E. L. Cussler. Hollow fiber modules made with hollow fiber fabric. *J. Membr. Sci.* 84:1–14, 1993.